Available online at www.sciencedirect.com
ScienceDirect
Analytica Chimica Acta 581 (2007) 303–308
ANALYTICA CHIMICA ACTA
www.elsevier.com/locate/aca

Laser-induced breakdown spectroscopy in analysis of Al^{3+} liquid droplets: On-line preconcentration by use of flow-injection manifold

Jer-Shing Huang [a,b], Hsiao-Tsui Liu [a,b], King-Chuen Lin [a,b,*]

[a] Department of Chemistry, National Taiwan University, Taipei 106, Taiwan
[b] Institute of Atomic and Molecular Sciences, Academia Sinica, Taipei 106, Taiwan

Received 25 April 2006; received in revised form 11 August 2006; accepted 22 August 2006
Available online 26 August 2006

Abstract

Laser-induced breakdown spectroscopy (LIBS), combined with a flow-injection system, is demonstrated to analyze liquid droplets of aluminum salt, as generated with an electrospray ionization device. The spray needle also serves as the anode, through which the analyte solution is spread toward the other metal base as the cathode. Along the passage of the FI manifold, the Al-sample loading speed is controlled at 0.15 mL min^{-1}, restricted to the small diameter of the spray needle, and the loading volume amounts to 0.1 mL. The metal ion is retained in a cation-exchange resin microcolumn immobilized with Chromotrope 2B chelating agent, followed by elution with a 0.5 M HCl solution into LIBS. Upon laser irradiation at the preconcentrated liquid droplets, the time-resolved laser-induced breakdown (LIB) emission and plasma-induced current signals are acquired concurrently on a single-shot basis. The area under the LIB/current distribution increases in linear proportion as the concentration of the sample solution increases. The detection limit thus obtained can reach 1.5 mg L^{-1}, about an order of magnitude lower than those achieved previously using single-laser ablation without involvement of preconcentration. The linear dynamic range is more than two orders of magnitude.

Keywords: Laser-induced breakdown spectroscopy; Preconcentration; Flow-injection: Liquid analysis

1. Introduction

Laser-induced breakdown spectroscopy (LIBS) is suitable for hostile environments [1], multi-elemental detection [2], minimal sample preparation, and non-invasive analysis. However, severe emission signal fluctuation reduces its sensitivity [3,4]. To suppress this signal fluctuation, the methods based on internal or external reference normalization have been widely developed [5–7]. As an external reference normalization, we have recently developed a correlation method based on plasma-induced current normalization analyzing the sample droplets [8–10]. The limit of detection (LOD) obtained for the alkali-elements analysis may reach <1 mg L^{-1} even with the addition of matrix salts up to 2000 mg L^{-1} [9].

Although applications of LIBS in liquid state are sparse, its development to analyze the liquid samples is crucial. For instance, LIBS installed with fiber-optics can offer an efficient remote analysis with minimal sample pretreatment to inspect trace metals in waste or contaminated ground water under hazardous environments [11]. There are some inherent disadvantages for the liquid LIBS analysis. The dissolved gas, solids and particulate materials from the samples easily cause misfocusing of the laser beam. When the system is exposed to the ambient condition, the air and produced matrices may feasibly pre-breakdown, thereby interfering severely with the LIBS signal of the analyte. Furthermore, the plasma-plume confinement by liquid and shortened lifetime of the excited state analyte make it impossible to separate LIB emission spatially [12–14] or temporally [10,15–17] from the continuum background, which is originated from the plasma central core. These shortcomings result in poor detection limit for the liquid samples. Application of a two-lasers technique [18–21], with one laser controlled for atomization process and the other for excitation, can effectively allow LIBS to avoid the temporal and spatial overlap with the continuum background, and subsequently to achieve a LOD comparable to those by modern atomic spectroscopy.

As an alternative and yet inexpensive method, the treatment with preconcentration may efficiently enhance the detection sensitivity of LIBS for the liquid samples. For instance, Vander

* Corresponding author at: Department of Chemistry, National Taiwan University, Taipei 106, Taiwan. Fax: +886 2 23621483.
E-mail address: kclin@ccms.ntu.edu.tw (K.-C. Lin).

0003-2670/$ – see front matter © 2006 Elsevier B.V. All rights reserved.
doi:10.1016/j.aca.2006.08.041

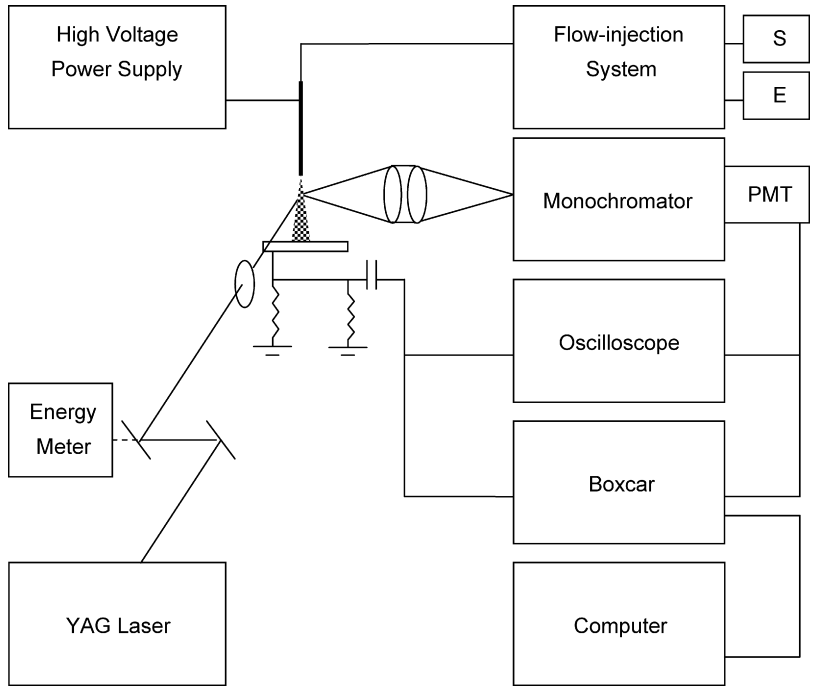

Fig. 1. Schematic diagram of FI-LIBS setup. The letter S denotes sample solution and E denotes eluent.

Wal et al. [22] dried the liquid sample on carbon substrates, which was analyzed under adjustable pressure of the ambient gas. The LOD for 15 elements was achieved ranging from 10 ng mL^{-1} to 10 μg mL^{-1}. Schmidt and Goode [23] immobilized the metal ions into an ion exchange polymer membrane, which was then ablated with a focused laser source. The multiple-element LIB analysis led to a LOD from 4 ng mL^{-1} to 2 μg mL^{-1}. They also used this technique for speciation of Cr(III) and Cr(VI) [24]. Despite success of these methods, to our knowledge, an on-line process of preconcentration followed by detection with LIBS has not yet been reported. This work is aimed to present such a method.

Herein, we develop a technique to couple LIBS with a flow-injection (FI) system. Along the FI passage, the Al metal ions are preconcentrated in a microcolumn packed with Chromotrope 2B-immobilized ion-exchange resin and then eluted through the electrospray ionization needle for detection with LIBS. In this manner, the LIB/current analysis for the Al salt may appreciably lower LOD and extend the linear dynamic range. A detailed data analysis, different from our previous LIB/current normalization, will be discussed.

2. Experimental

2.1. Setup of FI-LIBS

A schematic diagram for the LIBS system is illustrated in Fig. 1. In brief, a third harmonic Nd:YAG laser (DCR-2A, Spectra-Physics), operated at 10 Hz with duration 5–8 ns, emitting at 355 nm was used as the light source. The incident pulse was focused through a 10-cm focal length quartz lens onto the microdroplets generated by an electrospray ionization needle. The pulse energy prior to the quartz lens was controlled at 30 mJ, which was monitored constantly with an energy meter. The pulse-to-pulse fluctuation remained at ±5%.

A homemade electrospray ionization device was employed to generate a stream of microdroplets [8–10]. The analyte solution was syringe-pumped into a 200-μm i.d. stainless steel spray needle. The needle was biased at 3 kV as the anode, through which the analyte solution was sprayed toward the other metal base as the cathode. The analyte solution broke into droplets as carrier solvent evaporated. The laser pulse interacted with the sprayed droplets at ∼2 mm downstream from the needle tip. The irradiated spot was close to the tip of Taylor cone where a higher density of microdroplets may be gained. The produced luminous plume was imaged with a set of 15 and 20-cm focal length lenses onto a 0.22 m Czerney-Turner monochromator (Model 1680B, Jobin Yvon-SPEX), with a reciprocal dispersion of 18 Å mm^{-1} and a grating fixed at 396 nm, behind which a photomultiplier tube (PMT, 1P28A, Hamamatsu) was mounted. The acquisition of LIB emission at 396.2 nm corresponds to the $3p^2\ P_{3/2} \rightarrow 4s^2\ S_{1/2}$ transition of neutral Al atom, which yields the largest Einstein emission coefficient of $0.98 \times 10^8\ s^{-1}$ [25]. Although the initial state is the fine-structure excited level, it is above the fine-structure ground level $3p^2\ P_{1/2}$ by only 112 cm^{-1}. The time-resolved LIB signal was then fed into either a transient digitizer (Model 9450A, LeCroy) for single-shot profile recording or a boxcar integrator (Model SR250, Stanford Research System) for signal processing. The time-resolved spectra were integrated within a 4 μs gate, in 500 ns delay relative to the onset of the continuum background emission. Adjustment of the gate width and delay time may help suppress the LIB signal fluctuation to make the LIB emission the least interfered with by the intense continuum background. Note that the potential of 3 kV biased at the anode may not lead to any DC Stark splitting or broadening for the LIB emission signal. The produced charges are kept

removed away by the droplets such that the resultant electric field is not large enough. Nevertheless, the large biased potential may cause the movement of charged particles between the electrodes, thereby inducing a large current for collection. The potential adjustment depends on the distance between electrodes.

As in our previous work [8–10], the current profile in rapid oscillation was collected from the cathode via a high-pass filter into a second channel of either a transient digitizer or a boxcar integrator. Its first maximum peak, monitored concurrently with the LIB emission on a single-shot basis, was integrated within a 20 ns gate. To acquire a better LIB emission/current (LIB/C) correlation linearity, it must rely on an appropriate adjustment of the current gate width and position.

A 1000 mg L^{-1} aluminum chloride (Anhydrous, Reagent grade, Merck) solution was first prepared with water/methanol (v/v = 1:1) (HPLC grade, Baker) as solvent and then diluted to the desired concentrations. A water/methanol (v/v = 1:1) mixed solvent was used throughout this work for gaining a better electrospray efficiency. As packing materials in the microcolumn, AG1-X8 ion-exchange resin (100–200 mesh, Bio-Rad, Germany) and Chromotrope 2B (Acros Organics) were used from the purchase. The HCl eluent was made up for 0.5 M in water/methanol (v/v = 1:1) solution.

2.2. Column preparation and FI manifold

A AG1-X8 resin weighted at 1.0 g was added to a 25 mL aqueous solution with 10^{-2} mol Chromotrope 2B. The suspension in red was stirred about 50 min until the supernatant turned colorless with the blue resin settled. The immobilized resin was then transferred to a homemade Teflon microcolumn with 35 mm long × 5 mm i.d. Each end cap was stuffed with a filter < 3 μm pore size to prevent from the resin losses.

The FI manifold contained a syringe pump (Model KDS100, KD Scientific, USA), a microcolumn packed with Chromotrope 2B-bonded resin, and injection valves (1 four-way and 1 six-way). The two-channel syringe pump moved the sample and the eluent solutions simultaneously at the same speed of 0.15 mL min^{-1}. The pumping speed was restricted to the small diameter of electrospray ionization needle. At first, a 0.5 M HCl solution was eluted through the microcolumn to clean up the packed resin and the related passage. The sample solution bypassing the microcolumn was concomitantly loaded in the other channel of the FI manifold. Then, the four-way value was switched to guide this sample solution into LIBS for detection. The LOD thus obtained may be compared with that after preconcentration. Next, the six-way valve was turned to load the sample solution into the microcolumn for 40 s duration, corresponding to a volume of 0.1 mL. The Al^{3+} ion chelating with the Chromotrope 2B-immobilized resin was retained in the microcolumn, followed by elution into LIBS with a 0.5 M HCl solution.

3. Results and discussion

As a 100 mg L^{-1} Al salt solution is injected in the FI passage either bypassing or going through the microcolumn, a stream of single-shot time-dependent LIB emission spectra are acquired upon the laser irradiation at the sample microdroplets. The temporal profile begins with an intense peak, attributed to the continuum background, followed by a rise of Al LIB emission in hundreds of nanoseconds delay [8–10]. The LIB and the corresponding current profiles are integrated, respectively, within an individual gate. The resultant intensities up to 1000 data points are collected in Fig. 2.

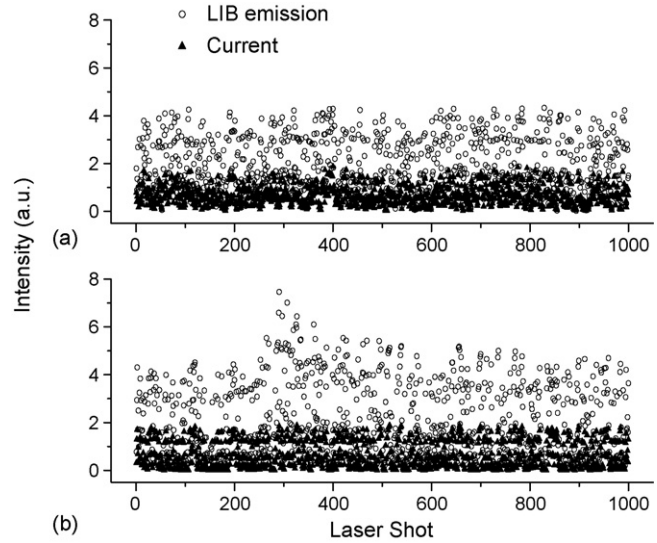

Fig. 2. The intensity distributions of LIB (◯) and current (▲) over 1000 data points, each denoting a profile area within a individual gate. (a) 100 mg L^{-1} Al salt solution without preconcentration treatment. (b) 100 mg L^{-1} Al salt solution with preconcentration treatment.

3.1. LIB/current correlation without preconcentration

For the case without preconcentration, despite fluctuation of the LIB intensities, they may be linearly correlated with the current intensities on a shot-to-shot basis. As shown in Fig. 3, the plot yields a straight line with a slope, which is sensitive to the

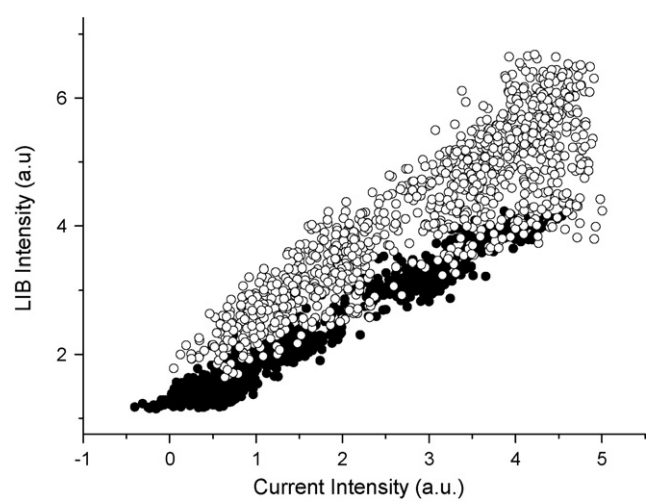

Fig. 3. Shot-to-shot correlation plot of LIB emission vs. plasma-induced current over 1000 laser shots. (●) 100 mg L^{-1} Al salt solution without preconcentration treatment. (◯) 100 mg L^{-1} Al salt solution as concentrated through the microcolumn.

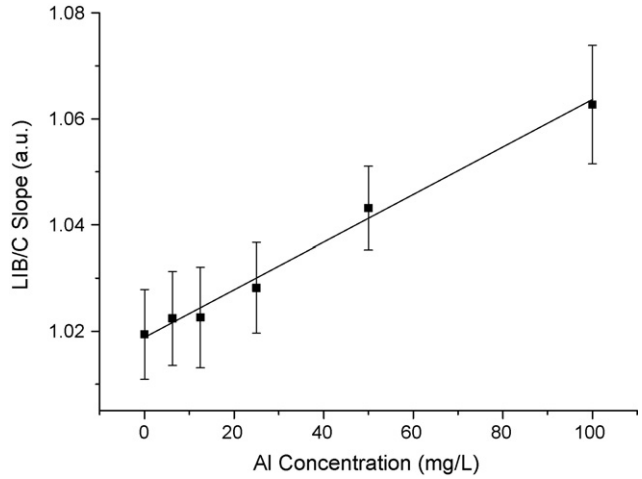

Fig. 4. Calibration curve for the Al concentration obtained with the correlation methods of LIB/current without preconcentration. Each error bar indicates the standard deviation of the slope in the plot of LIB vs. current for 200 data points.

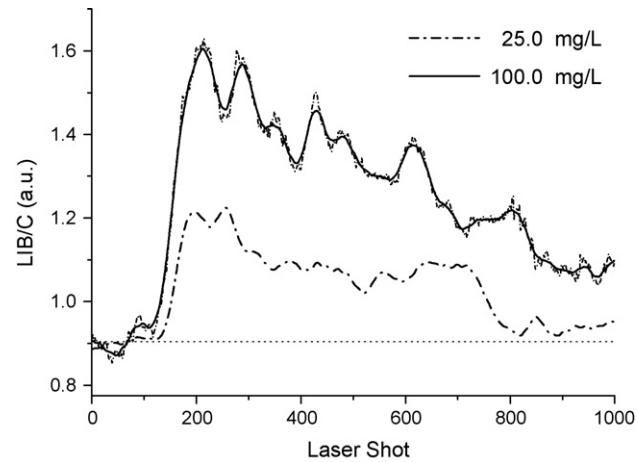

Fig. 5. The ratio distributions of LIB/current for the initial concentrations at 25 and 100 mg L^{-1}. The bold line indicates the average over the adjacent 30 data points. The dashed line indicates the baseline determined from the early about 50 data points, which are attributed to the blank solution.

concentration variation. The linear relationship implies that the emission signals result substantially from the breakdown events, rather than the laser-induced excitation/emission with which the plasma-induced current may otherwise exhibit random correlation.

As shown in Fig. 4, the slopes obtained in the LIB/current plots as a function of the sample concentration give rise to a calibration curve, which is quantitatively described by a regression equation, yielding $Y \pm 0.204 = (1.019 \pm 0.005) + (4.49 \pm 1.20) \times 10^{-4} X$ with a regression coefficient, R, of 0.994. Each error bar indicates the standard deviation of the slope in the plot of LIB versus current for 200 data points. Note that the calibration curve does not pass through the origin point. It is caused by the fact that the correlation slope for the blank solution is not zero, suggesting that the LIB emission and the continuum background may not be temporally demarcated completely. The small, non-zero background, equally contributing to all the concentration measurements, does not affect the determination of sensitivity of the calibration curve. Given the sensitivity of the calibration curve, $m = 4.49 \times 10^{-4}$, and the standard deviation of the blank solution, $\sigma = 0.0086$, obtained from the slope of correlation plot, LOD defined as $2\sigma/m$, reaches 38 mg L^{-1} for the Al sample. As compared to the LOD determined for alkali elements, the Al detection limit appears to be worse by about one to two orders of magnitude [8].

3.2. LIB/current correlation with preconcentration

The shot-to-shot distributions for the case with preconcentration (Fig. 2b) look similar to those without preconcentration (Fig. 2a), but the LIB intensities rise to peak at about 300 laser shots and then decrease gradually. The feature of peak broadening and tailing is caused by the concentration dispersion along the FI passage, as a result of complicated diffusion and pressure effect as in a chromatogram. In contrast, the current intensities remain within the same regular range, independent of the concentration variation. The plasma-induced current is substantially attributed to the collected electrons mainly from the ionized water/methanol droplets and their fragments [8]. The current response thus obtained is proportional to both the ablated droplet sizes and the electron motion, but irrespective of the sample concentration contained. Increasing the sample concentration may increase the LIB emission intensity, but does not change the current response significantly.

While plotting LIB intensities against current intensities over these 1000 data points, Fig. 3 shows a broad spread of distribution, instead of a straight line. Since the correlation slope depends on the concentration, such a distribution may be considered as superposition of a number of slopes caused by the concentration variation. If such correlation slopes are used to gain the calibration curve, as describe above, two shortcomings may appear. First, the slope of the correlation plot must bear a large standard deviation. Second, the slope does not change markedly with the concentration such that the obtained calibration curve may have a small sensitivity.

Instead, we analyze the results given in Fig. 2b by plotting a LIB/current distribution over the 1000 data points. As shown in Fig. 5, it resembles the LIB distribution of Fig. 2b. Even though the current normalization is considered, the ratio fluctuates severely. For minimizing the fluctuation, the ratio distribution is smoothed in such a way to replace original data point with an average over the adjacent 30 data points (Fig. 5). In the early about 50 data points, the LIB emission results from the flow of the pure HCl solution in which the Al sample has not been blended yet. Thus this portion attributed to the blank solution may well be adopted as a baseline. Then, the LIB emission rises to the peak as the sample is concentrated. Fig. 5 also shows that the LIB/current distribution increases with increasing the initial concentration. The integrated area of the entire profile, after subtracting the area under the baseline, leads to intimate correlation with the initial concentration. As shown in Fig. 6, a calibration curve is fitted accordingly with a regression coefficient, $R = 0.999$, by using the regression equation of $Y \pm 1.83 = (0.67 \pm 2.05) + (4.28 \pm 0.06)X$, in which X and Y

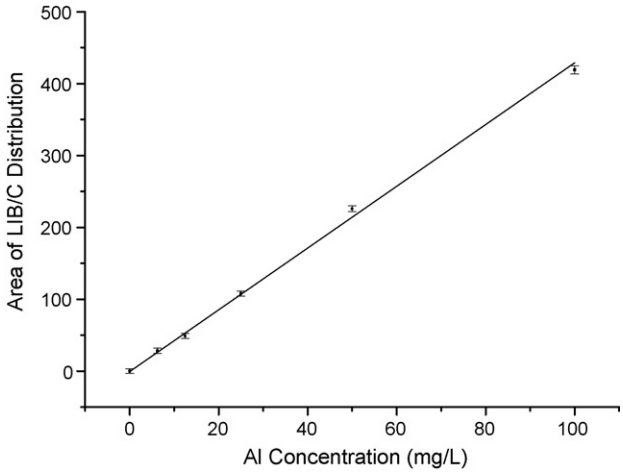

Fig. 6. Calibration curve for the Al sample solution as concentrated through the microcolumn. The integrated areas of LIB/current distributions over 1000 data points are plotted as a function of the initial concentration. Each error bar indicates an average of three replicates.

denote the Al^{3+} concentration and the area of LIB/C distribution over 1000 data points, respectively. Each error bar indicates an average of three replicates, different definition from that given in Fig. 4. LOD is evaluated by $2\sigma/m$, in which σ, the error bar of the blank solution, is measured of 3.25, and m, the sensitivity of the calibration curve, is determined above. Thus, LOD reaches 1.5 mg L^{-1} for the Al sample at the laser energy 30 mJ. Although further improvement by increasing the laser energy is not tried, this result is about an order of magnitude better than those achieved previously using single-laser ablation without preconcentration [8,13,26–28]. The dynamic range reaches at least two orders of magnitude, from 1.5 mg L^{-1} to 100 mg L^{-1}, larger than the other case shown in Fig. 4.

3.3. Advantages of LIB/current correlation

Development of the LIB/current correlation technique provides several advantages. First, the method has taken into account the ablated amount of microdroplets and the plasma excitation temperature. Therefore, the correlation linearity may be achieved over a much wider range of laser energy and lead to a better sensitivity and lower LOD for a liquid sample analysis, as compared to the LIB/background normalization [10]. Second, despite irregular shapes of the droplets and frequent occurrence of laser misfocusing, the current normalization may reach a low level of LOD, comparable to those obtained with other external reference normalization, and yet gaining an even smaller absolute quantity of the sample contents [8]. Third, the method is free from interference by the matrix salt effect. The electrons, responsible for the current intensity, are collected substantially from the ionized water/methanol droplets and their fragments, while little from the contained sample or matrix salts. Thus increase of the matrix salts may not suppress the LIB intensity [9]. Therefore, in case some coexisting ions have similar combination ability with Chromotrope 2B chelating agent in this work, the resultant matrix influence may not cause any significant interference with the LIB/current correlated signals. The calibration curve and the subsequent LOD determination may not be significantly deviated. Finally, the electrospray ionization needle is suitable for a FI-manifold coupling to make use of the on-line preconcentration and separation merits, thereby the detection sensitivity may be further enhanced.

4. Conclusion

We have recently developed a LIB/current correlation method for analysis of the liquid droplets. In this work, we take a further step to incorporate a FI system with LIBS. The sprayed droplets of the Al salt, preconcentrated along the passage of the FI manifold, are ablated with the focused laser beam at 355 nm. Then, the time-resolved LIB profile and the plasma-induced current signal are acquired concurrently. Unlike the peak narrowness shown in a chromatogram, the distribution of the LIB/current ratios on the single-shot basis is characteristic of broadening and tailing. Nevertheless, the profile areas exhibit a linear dependence on the sample concentration. The dynamic range reaches at least two orders of magnitude, from 1.5 mg L^{-1} to 100 mg L^{-1}, and the LOD is lowered by 20-fold. In addition to the preconcentration advantage, the present method makes use of the separation merit provided by the FI manifold, removing most matrix salts before acquisition of the LIB emission signal. Despite active focus of this work on the standard solutions, we may well believe that this technique will be free from the matrix interference if reference materials are examined [9].

Acknowledgement

This work is supported by the National Science Council of the Republic of China under contract no. NSC93-2113-M-002-028.

Appendix A. Supplementary data

Supplementary data associated with this article can be found, in the online version, at doi:10.1016/j.aca.2006.08.041.

References

[1] B. Salle, J.L. Lacour, E. Vors, P. Fichet, S. Maurice, D.A. Cremers, R.C. Wiens, Laser-induced breakdown spectroscopy for Mars surface analysis: capabilities at stand-off distances and detection of chlorine and sulfur elements, Spectrochim. Acta, Part B 59 (2004) 1413–2142.
[2] D. Romero, J.J. Laserna, Multielemental chemical imaging using laser-induced breakdown spectrometry, Anal. Chem. 69 (1997) 2871–2876.
[3] J.D. Winefordner, I.B. Gornushkin, T. Correll, E. Gibb, B.W. Smith, N. Omenetto, Comparing several atomic spectrometric methods to the super stars: special emphasis on laser induced breakdown spectrometry, LIBS, a future super star, J. Anal. At. Spectrom. 19 (2004) 1061–1083.
[4] M. Capitelli, A. Casavola, G. Colonna, A. De Giacomo, Laser-induced plasma expansion: theoretical and experimental aspects, Spectrochim. Acta, Part B 59 (2004) 271–289.
[5] L. Xu, V. Bulatov, V.V. Gridin, I. Schechter, Absolute analysis of particulate materials by laser-induced breakdown spectroscopy, Anal. Chem. 69 (1997) 2103–2108.
[6] N.H. Cheung, E.S. Yeung, Single-shot elemental analysis of liquids based on laser vaporization at fluences below breakdown, Appl. Spectrosc. 47 (1993) 882–886.

[7] C. Chaleard, P. Mauchien, N. Andre, J. Uebbing, J.L. Lacour, C. Geertsen, Correction of matrix effects in quantitative elemental analysis with laser ablation optical emission spectrometry, J. Anal. At. Spectrom. 12 (1997) 183–188.
[8] J.S. Huang, C.B. Ke, L.S. Huang, K.C. Lin, The correlation between ion production and emission intensity in the laser-induced breakdown spectroscopy of liquid droplets, Spectrochim. Acta, Part B 53 (2002) 35–48.
[9] J.S. Huang, C.B. Ke, K.C. Lin, Matrix effect on emission/current correlated analysis in laser-induced breakdown spectroscopy of liquid droplets, Spectrochim. Acta, Part B 59 (2004) 321–326.
[10] J.S. Huang, K.C. Lin, Laser-induced breakdown spectroscopy of liquid droplets: correlation analysis with plasma-induced current versus continuum background, J. Anal. At. Spectrom. 20 (2005) 53–59.
[11] W.B. Lee, J.Y. Wu, Y.I. Lee, J. Sneddon, Recent applications of laser-induced breakdown spectrometry: a review of material approaches, Appl. Spectrosc. Rev. 39 (2004) 27–97.
[12] J.D. Hybl, G.A. Lithgow, S.G. Buckley, Laser-induced breakdown spectroscopy detection and classification of biological aerosols, Appl. Spectrosc. 57 (2003) 1207–1215.
[13] F. Courvoisier, V. Boutou, C. Favre, S.C. Hill, J.P. Wolf, Plasma formation dynamics within a water microdroplet on femtosecond time scales, Opt. Lett. 28 (2003) 206–208.
[14] J.A. Aguilera, J. Bengoechea, C. Aragón, Curves of growth of spectral lines emitted by a laser-induced plasma: influence of the temporal evolution and spatial inhomogeneity of the plasma, Spectrochim. Acta, Part B 58 (2003) 221–237.
[15] F. Colao, S. Pershin, V. Lazic, R. Fantoni, Investigation of the mechanisms involved in formation and decay of laser-produced plasmas, Appl. Surf. Sci. 197 (2002) 207–212.
[16] I.B. Gornushkin, C.L. Stevenson, B.W. Smith, N. Omenetto, J.D. Winefordner, Modeling an inhomogeneous optically thick laser induced plasma: a simplified theoretical approach, Spectrochim. Acta, Part B 56 (2001) 1769–1785.
[17] I.B. Gornushkin, B.W. Smith, G.E. Potts, N. Omenetto, J.D. Winefordner, Some considerations on the correlation between signal and background in laser-induced breakdown spectroscopy using single-shot analysis, Anal. Chem. 71 (1999) 5447–5449.
[18] D.C.S. Beddows, O. Samek, M. Liska, H.H. Telle, Single-pulse laser-induced breakdown spectroscopy of samples submerged in water using a single-fibre light delivery system, Spectrochim. Acta, Part B 57 (2002) 1461–1471.
[19] V.N. Rai, F.Y. Yueh, J.P. Singh, Study of laser-induced breakdown emission from liquid under double-pulse excitation, Appl. Opt. 42 (2003) 2094–2101.
[20] S.K. Ho, N.H. Cheung, Sub-part-per-billion analysis of aqueous lead colloids by ArF laser induced atomic fluorescence, Anal. Chem. 77 (2005) 193–199.
[21] A. Kuwako, Y. Uchida, K. Maeda, Supersensitive detection of sodium in water with use of dual-pulse laser-induced breakdown spectroscopy, Appl. Opt. 42 (2003) 6052–6056.
[22] R.L. Vander Wal, T.M. Ticich, J.R. West, P.A. Householder, Trace metal detection by laser-induced breakdown spectroscopy, Appl. Spectrosc. 53 (1999) 1226–1236.
[23] N.E. Schmidt, S.R. Goode, Analysis of aqueous solutions by laser-induced breakdown spectroscopy of ion exchange membranes, Appl. Spectrosc. 56 (2002) 370–374.
[24] C.R. Dockery, J.E. Pender, S.R. Goode, Speciation of chromium via laser-induced breakdown spectroscopy of ion exchange polymer membranes, Appl. Spectrosc. 59 (2005) 252–257.
[25] W.L. Wiese, M.W. Smith, B.M. Miles, Atomic transition probabilities, V.II, National Stand. Ref. Data Ser. Nat. Bur. Stand. 22 (U.S. Department of Commerce), 1969. p. 48.
[26] P. Fichet, P. Mauchien, J. Wagner, C. Moulin, Quantitative elemental determination in water and oil by laser induced breakdown spectroscopy Anal, Chim. Acta 429 (2001) 269–278.
[27] D.A. Cremers, L.J. Radziemski, T.R. Loree, Spectrochemical analysis of liquids using the laser spark, Appl. Spectrosc. 38 (1984) 721–729.
[28] C.W. Ng, W.F. Ho, N.H. Cheung, Spectrochemical analysis of liquids using laser-induced plasma emissions: Effects of laser wavelength on plasma properties, Appl. Spectrosc. 51 (1997) 976–983.